ISBN: 978-3-95450-233-2 ISSN: 2673-5504 doi:10.18429/JACoW-SRF2021-SUPFDV003

EFFECT OF MEAN FREE PATH ON NONLINEAR LOSSES OF TRAPPED VORTICES DRIVEN BY A RF FIELD*

W.P.M.R Pathirana†, Alex Gurevich
Center for Accelerator Science, Old Dominion University, Norfolk, USA

Abstract

We report extensive numerical simulations on nonlinear dynamics of a trapped elastic vortex under rf field, and its dependence on electron mean free path l_i. Our calculations of the field-dependent residual surface resistance $R_i(H)$ take into account the vortex line tension, the linear Bardeen-Stephen viscous drag and random distributions of pinning centers. We showed that $R_i(H)$ decreases significantly at small fields as the material gets dirtier while showing field independent behavior at higher fields for clean and dirty limit. At low frequencies $R_i(H)$ increases smoothly with the field amplitude at small H and levels off at higher fields. The mean free path dependency of viscosity and pinning strength can result in a nonmonotonic mean free path dependence of R_i, which decreases with l_i at higher fields and weak pinning strength.

INTRODUCTION

RF losses in SRF cavities are quantified by the quality factor Q_0 which is inversely proportional to the surface resistance R_s. The surface resistance consists of two parts, $R_s = R_{BCS} + R_i$, where $R_{BCS} \propto \omega^2 \exp(-\Delta/T)$ comes from thermally activated quasiparticles while R_i quantified a weakly-temperature dependent residual resistance. The temperature independent R_i can produce a large fraction of the total dissipation about $\approx$ 20% for Nb and $\approx$ 50% for Nb_3Sn at 2 K and 1-2 GHz [1]. So the dependence of R_i on the magnetic field H, frequency f and mean free path (l_i) is of much interest. The main contributions to R_i comes from trapped vortices generated during the cavity cool down through the critical temperature T_c at which the lower critical field $H_{c1}(T)$ vanishes [2–10]. In this case even small stray fields $H > H_{c1}(T)$ such as unscreened earth magnetic field can produce vortices in the cavity. During the subsequent cooldown to $T \simeq 2$ K some of these vortices exit the cavity but some get trapped by the material defects such as non-superconducting precipitates, network of dislocations or grain boundaries.

Low-field rf losses of pinned vortices have been calculated by many authors [3, 11–15]. Nonlinear quasi-static electromagnetic response of perpendicular vortices has been addressed both for weak collective pinning [1], and strong pinning [16, 17]. The extreme nonlinear dynamics of a vortex under a strong ac magnetic field at which $R_i(H)$ decreases with H because of the decrease of vortex viscosity with the velocity was addressed in [18]. The dissipation of vortices under a strong magnetic field in the cases of mesoscopic pinning has been calculated recently by [19]. The nonlinear dynamics of the trapped vortex and the field dependence R_i can also be tuned by nonmagnetic impurities. Yet, the mean free path dependency of the rf power generated by flexible oscillating vortex though a random pinning potential remains poorly understood. In this work, we calculate field dependent $R_i(H)$ and its dependencies on the mean free path, frequency and the pinning strength due to a trapped vortex line under rf magnetic field. Our calculation take into account the vortex line tension, pinning force, and Bardeen-Stephen viscous drag force.

DYNAMIC EQUATIONS

Consider a single vortex pinned by materials defects as shown in the Fig. 1. Here the vortex is driven by the ac

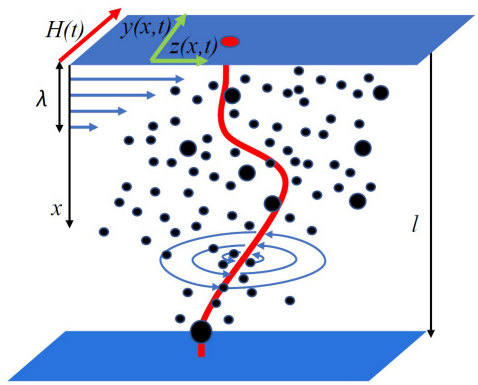

Figure 1: A flexible vortex shown by the read line driven by the rf surface current. The black dots represent pinning centers such as non-superconducting precipitates. Green arrows show vortex tip displacement on the YZ plane.

Meissner currents flowing in a thin layer of $\sim \lambda$ at the surface. The ac displacement of the vortex $\mathbf{R} = [Y(X,t), Z(X,t)]$ is mainly confined within the elastic skin depth [3] so that the vibrating vortex segment interacts only with a few pins while the rest of the vortex does not move. In this situation, the electromagnetic response of a perpendicular vortex becomes dependent on its position and the statistical distribution of random pinning potentials. For instance, Fig.1 shows a representative case of bulk pinning by small, randomly-distributed non-superconducting precipitates. The dynamic equation for trapped vortex shown in the Fig. 1 is given by:

$$M\frac{\partial^2 \mathbf{R}}{\partial t^2} + \eta\frac{\partial \mathbf{R}}{\partial t} = \epsilon\frac{\partial^2 \mathbf{R}}{\partial X^2} - \nabla U(X,\mathbf{R}) - \hat{y} f_L(X,t), \quad (1)$$

$$f_L(X,t) = (\phi_0 H/\lambda) e^{-X/\lambda} \sin\omega t, \quad (2)$$

* This work was supported by NSF under Grant 100614-010 and Grant 1734075.
† mwali003@odu.edu

ISBN: 978-3-95450-233-2 ISSN: 2673-5504 doi:10.18429/JACoW-SRF2021-SUPFDV003

where H is the amplitude of the applied magnetic field with the frequency f , λ is the London penetration depth, M is the vortex mass per unit length, $\epsilon = \phi_0^2(\ln\kappa + 0.5)/4\pi\mu_0\lambda^2$ is the vortex line energy, $\kappa = \lambda/\xi$ is the Ginzburg-Landau (GL) parameter, ξ is the coherence length, and η is the viscous drag coefficient. Equations (1) and (2) represent a balance of local forces acting on a curvilinear vortex: the inertial and viscous drag forces in the left hand side are balanced by the elastic, pinning and Lorentz forces in the right hand side. It is assumed that: 1. The field is well below the superheating field [20–23] so that the London model is applicable. 2. The Magnus force causing a small Hall angle [24–26] is negligible. 3. The low frequency rf field ($\hbar\omega \ll \Delta$) does not produce quasiparticles, and the quasi-static London equations are applicable [27]. 4. Bending distortions of the vortex are small so the linear elasticity theory [11, 28] is applicable. We consider here the core pinning of vortices [11,28,29] represented by a sum of pinning centers modeled by the Lorentzian functions [30]:

$$U(X,\mathbf{R}) = -\sum_{n=1}^{N} \frac{U_n}{1+[(X-X_n)^2+|\mathbf{R}-\mathbf{R}_n|^2]/\xi^2}. \quad (3)$$

Here, X_n, Y_n and Z_n are the coordinates of the n-th pinning center, and U_n are determined by the gain in the condensation energy in the vortex core at the pin [11,28,29]. To take into account dependencies of superconducting parameters on the mean free path l_i in Eqs. (1)-(3), we used $\rho_n \propto l_i^{-1}$ and the conventional GL interpolation formulas $\lambda = \lambda_0\Gamma$, and $\xi = \xi_0/\Gamma$, where $\Gamma = (1+\xi_0/l_i)^{1/2}$. As a result, we obtain the following dimensionless nonlinear partial differential equations for the local coordinates $y(x,t) = Y/\lambda_0$ and $z(x,t) = Z/\lambda_0$:

$$\gamma\dot{y} = y'' - \sum_{n=1}^{N} A_n(x,\mathbf{r})(y-y_n) + \beta_t e^{-x/\Gamma}, \quad (4)$$

$$\gamma\dot{z} = z'' - \sum_{n=1}^{N} A_n(x,\mathbf{r})(z-z_n), \quad (5)$$

$$y'(0,t) = z'(0,t) = y'(l,t) = z'(l,t) = 0. \quad (6)$$

Here the prime and the dot imply differentiation over the dimensionless coordinate $x = X/\lambda_0$ and time $t = tf$, respectively, the vortex mass is neglected. $\mathbf{r} = [y(x,t), z(x,t)]$, and:

$$\gamma = \frac{g_0\Gamma^4 l_i f}{g\xi_0 f_0}, \qquad f_0 = \frac{H_{c10}\rho_{n0}}{H_{c20}\lambda_0^2\mu_0}, \quad (7)$$

$$\beta_t = \beta\sin(2\pi t), \qquad \beta = \frac{g_0\Gamma H}{gH_{c10}}, \quad (8)$$

$$A_n = \frac{g_0\Gamma^5\zeta_{n0}}{g\left[1+\Gamma^2\kappa_0^2(x-x_n)^2+\Gamma^2\kappa_0^2|\mathbf{r}-\mathbf{r}_n|^2\right]^2}, \quad (9)$$

$$\zeta_{n0} = 2\kappa_0^2 U_n/\epsilon_0, \quad (10)$$

$$g_0 = \ln\frac{\lambda_0}{\xi_0} + \frac{1}{2}, \qquad g = \ln\frac{\lambda_0\Gamma^2}{\xi_0} + \frac{1}{2}. \quad (11)$$

where λ_0, ξ_0, ϵ_0, ρ_{n0}, $H_{c10} = (\phi_0/4\pi\mu_0\lambda_0^2)(\ln\kappa_0 + 0.5)$ and $H_{c20} = \phi_0/2\pi\mu_0\xi_0^2$ are the the penetration depth, coherence length, vortex line energy, normal-state resistivity, lower and upper critical fields in the clean limit, respectively. The amplitude U_n is related to the elementary pinning energy by $u_p = \pi\xi U_n$, so that $\zeta_n = 2\kappa^2 u_p/\pi\epsilon\xi = g_0\Gamma^5\zeta_{n0}/g$ as u_p is independent of mean free path [14].

We first estimate γ and ζ_n for a dirty Nb with $\lambda_0 = \xi_0 = 40$ nm and $U_n = 1.4$ meV/nm. Hence, $\gamma_0 = g_0 f/f_0 \approx 0.004$, and $\zeta_{n0} \simeq 0.04$ at $f = 1$ GHz. Another essential parameter is the decay length L_ω of oscillating bending disturbance along the vortex line induced by a weak rf current at the surface [3]

$$L_\omega = \sqrt{\frac{\epsilon}{\eta\omega}} = \frac{\lambda}{\sqrt{2\pi\gamma}}, \quad (12)$$

For Nb_3Sn, we have $L_\omega \simeq 5.15\lambda = 572$ nm at 1 GHz. In this case, dissipative oscillations of the elastic vortex extend well beyond the rf field penetration depth.

The power of rf losses is obtained by summing contributions of all vortices, $P = \sum_k \int\langle J(X,t)\partial_t Y_k(X,t)dX\rangle$, where $Y_k(X,t)$ describes the $k-$th vortex and $\langle..,\rangle$ means time averaging (see Ref. [19]). It is convenient to define a mean dimensionless power $p = P/P_0$ and the surface resistance r_i per vortex:

$$p = \frac{\gamma_0}{g_0\Gamma N_v}\sum_{k=1}^{N_v}\int_0^1 dt\int_0^l \beta_t e^{-x}\dot{y}_k(x,t)dx, \quad (13)$$

$$r_i(\beta) = 2p(\beta)/\beta^2, \quad (14)$$

where $P_0 = \lambda_0 f_0\epsilon_0$ and N_v is the number of vortices. The dimensionless r_i is related to the surface resistance R_i which defines the power losses per unit area $P = R_i H^2/2$ by $R_i = P_0 r_i n_\square/H_{c10}^2$. Here $n_\square = B_0/\phi_0$ is a vortex areal density producing a small induction $B_0 \ll B_{c1}$. Using here f_0 from Eq. (7) and $\epsilon_0 = \phi_0 H_{c10}$, we obtain:

$$R_i = \frac{\rho_{n0}B_0}{\lambda_0 B_{c20}} r_i. \quad (15)$$

NUMERICAL RESULTS

We solved Eqs. (4)-(6) numerically using COMSOL [31]. In our simulations, a straight vortex was initially put in a particular pinning potential, and after $\mathbf{r}(x,t)$ relaxes to a stable shape, the rf field was turned on. Then we run the program until $\mathbf{r}(x,t)$ reaches steady-state oscillations after a transient period $\delta t \lesssim 90/f$ and use this solution to calculate R_i. For the case of bulk pinning N identical pins were distributed randomly in a $l\times l_y\times l_z$ box and Eqs. (4)-(6) were solved for different mean free path, frequency, and rf field amplitudes, making sure that l_y and l_z are adjusted in such a way that the vortex always remains within the box during the rf period. The mean pin density $n_i = N/ll_y l_z$ was fixed through out the simulations.

Shown in Fig. 2 are the dependencies of the surface resistance $r_i(\beta)$ on the field amplitude $\beta = H/H_{c1}$ calculated for different mean free path values at $\kappa_0 = 2$. Here r_i is nearly

ISBN: 978-3-95450-233-2 ISSN: 2673-5504 doi:10.18429/JACoW-SRF2021-SUPFDV003

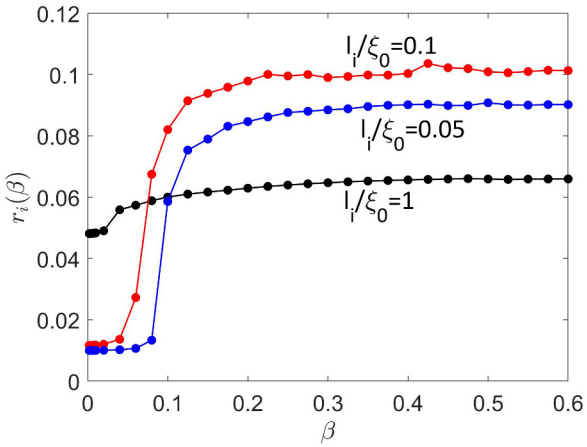

Figure 2: Field dependence of $r_i(\beta)$ calculated for different mean free path at $\kappa_0 = 2$ and $\zeta_{n0} = 0.04$. Other parameters are $l/\lambda_0 = 10$, $\gamma_0 = 0.004$, $n_i = 0.5\lambda_0^{-3}$.

independent of H at the higher field but develops a field dependence at smaller field values. As the mean free path is reduced $r_i(\beta)$ starts to decreases at small fields but increases as the field increases. This low field behavior is because L_ω decreases as l_i decreases, and the vortex interacts with small number of pins resulting in a lower surface resistance. The $r_i(\beta)$ at higher fields is mostly limited by the vortex drag, and the effect of pinning fluctuations weakens, resulting a field-independent behavior. As l_i decreases, the transition to flux flow regime from pinning regime occurs at a higher field because of higher pinning strength $\zeta_n \propto \Gamma^5$. For instance this transition occurs at $\beta \sim 0.1$ for $l_i/\xi_0 = 0.05$ but $\beta \sim 0.04$ for $l_i/\xi_0 = 1$. Curiously, $r_i(\beta)$ at $l_i/\xi = 0.05$ is slightly smaller than at $l_i/\xi_0 = 0.1$. Figure 3 shows the field depen-

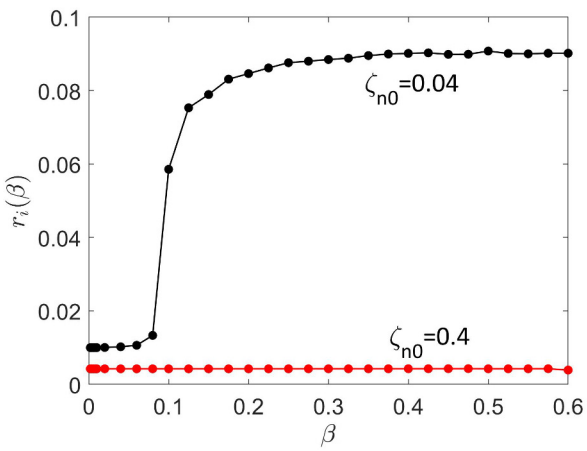

Figure 3: Surface resistance $r_i(\beta)$ calculated for different pinning strength $\zeta_{n0} = 0.04, 0.4$ at $l/\lambda_0 = 10$, $\gamma_0 = 0.004$, $n_i = 0.5\lambda_0^{-3}$, $l_i/\xi_0 = 0.05$ and $\kappa_0 = 2$.

dencies of $r_i(\beta)$ for bulk pinning calculated at two values of the pinning parameter ζ_n. The surface resistance $r_i(\beta)$ for weak pinning with $\zeta_n = 0.04$, increases sharply above $\beta \simeq 0.1$ due to the rapid transition from pinning regime to flux flow regime while strong pinning with $\zeta_n = 0.4$ stays approximately independent from the field as its depinning field $\beta_p(\zeta_{n0} = 0.4) >> \beta_p(\zeta_{n0} = 0.04)$ which can be calculated approximately using $\beta_p \simeq (\zeta_n \lambda/\kappa^2)\sqrt{n_i l} \sim 0.6$ [19] at $\zeta_{n0} = 0.4$ and $\beta_p \sim 0.06$ for $\zeta_{n0} = 0.04$. This restricts the motion of the vortex and results in a lower $r_i(\beta)$ at strong pinning.

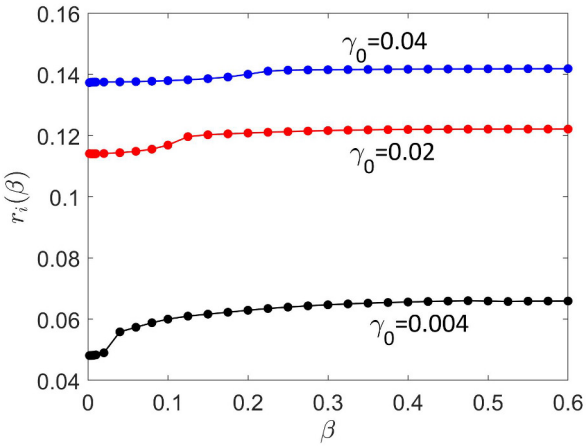

Figure 4: Surface resistance $r_i(\beta)$ calculated for different frequencies $\gamma_0 = 0.004, 0.02, 0.04$ at $l/\lambda_0 = 10$, $n_i = 0.5\lambda_0^{-3}$, $\kappa_0 = 2$, $l_i/\xi = 1$ and $\zeta_{n0} = 0.04$.

Now we turn to the effect of pinning on the frequency dependence on $r_i(\beta, \gamma)$ shown in Fig. 4. At a high frequency $\gamma = 0.4$ the surface resistance $r_i(\beta)$ is nearly independent of the field amplitude β because the rf losses are dominated by the linear vortex drag. As the frequency decreases, a linear dependence of $r_i(\beta)$ develops at small fields for which pinning reduces $r_i(\beta)$. This result is consistent with the calculations of $r_i(\beta)$ in a quasi-static limit [1].

Shown in Fig. 5 are the dependencies of the surface resistance $r_i(l_i)$ on the mean free path calculated at two different filed amplitude and κ_0. The peak in $r_i(l_i)$ shown in Fig. 5 (a) results from the interplay of the decrease of the vortex viscosity $\eta(l_i)$ and increase of pinning strength ζ_n as the vortex line gets softer in the dirty limit. Such a bell-shaped dependence of $r_i(l_i)$ has been observed experimentally [14, 15]. As the rf field amplitude β increases, the peak shifts to a lower mean path value. However, the opposite situation occurs at $\kappa_0 = 10$ shown in Fig. 5 (b). Here the dip in $r_i(l_i)$ occurs because the pinning strength parameter ζ_n increases significantly as l_i decreases, resulting in a lower r_i at small l_i. At higher field $\beta = 0.1$ which exerts larger Lorentz forces, pinning becomes less effective $r_i(l_i)$ shown in Fig. 5 (b) becomes similar to $r_i(l_i)$ shown in Fig. 5 (a) at $\kappa_0 = 2$.

CONCLUSION

We presented the numerical simulations of nonlinear dynamics of a single vortex moving in random pinning potentials under rf magnetic field. The power dissipated by an

ISBN: 978-3-95450-233-2 ISSN: 2673-5504 doi:10.18429/JACoW-SRF2021-SUPFDV003

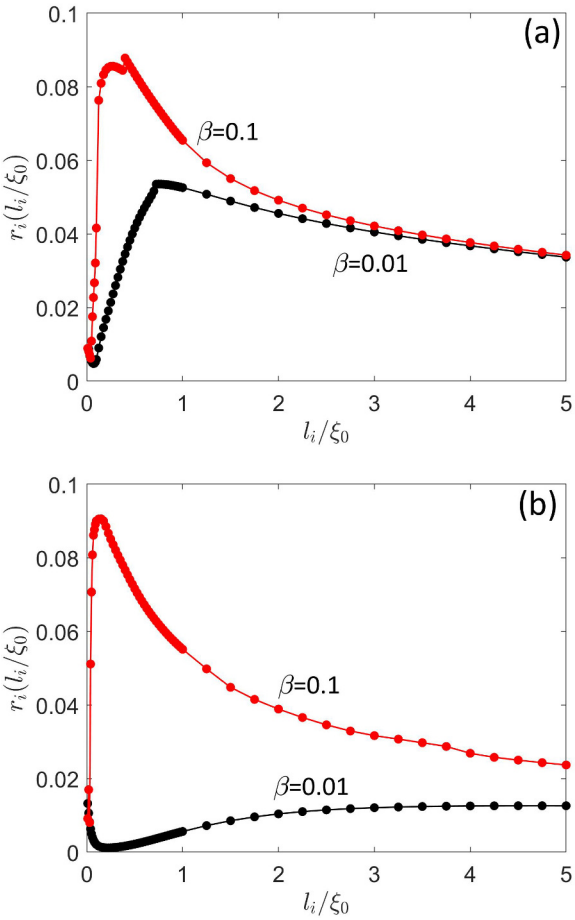

Figure 5: Mean free path dependencies of $r_i(l_i)$ calculated at $l/\lambda_0 = 10$, $n_i = 1.67\lambda_0^{-3}$, $\gamma_0 = 0.004$, $\beta = 0.01$ and $\beta = 0.1$, (a) $\kappa_0 = 2$, $\zeta_{n0} = 0.04$ (b) $\kappa_0 = 10$, $\zeta_{n0} = 1$.

oscillating vortex segment was calculated considering the line tension of the vortex, Bardeen-Stephen viscous drag force, and random pinning force with constant mean pin density at different rf fields amplitudes, mean free path, pinning strength and frequency. At low frequencies $R_i(H)$ gradually increases with the field at a small field, but as the frequency increases $R_i(H)$ becomes field independent. The field-dependent residual surface resistance decreases significantly at the small field in dirty material but shows a field-independent behavior at a higher field. We obtained a bell-shaped dependence of the surface resistance on the mean free path due to the interplay between the pinning and viscous forces.

ACKNOWLEDGMENTS

This work was supported by NSF under Grant 100614-010 and Grant 1734075.

REFERENCES

[1] D. B. Liarte, D. Hall, P. N. Koufalis, A. Miyazaki, A. Senanian, M. Liepe, J. P. Sethna, "Vortex dynamics and losses due to pinning: Dissipation from trapped magnetic flux in resonant superconducting radio-frequency cavities," *Appl. Phys. Rev.*, vol. 10, p. 054057, 2018.

[2] J-M. Vogt, O. Kugeler, J. Knobloch, "Impact of cool-down conditions at T_c on the superconducting rf cavity quality factor," *Phys. Rev. ST Accel. Beams,* vol. 16, p. 102002, 2013.

[3] A. Gurevich, and G. Ciovati, "Effect of vortex hot spots on the radio-frequency surface resistance of superconductors", *Phys. Rev. B,* vol. 87, p. 054502, 2013.

[4] A. Romanenko, A. Grassellino, O. Melnychuk, D. A. Sergatskov, "Dependence of the residual surface resistance of superconducting radio frequency cavities on the cooling dynamics around T_c," *J. Appl. Phys.,* vol. 115, p. 184903, 2014.

[5] D. Gonnella, R. Eichhorn, F. Furuta, M. Ge, D. Hall, V. Ho, G. Hoffstaetter, M. Liepe, T. O'Connell, S. Posen, P. Quigley, J. Sears, V. Veshcherevich, A. Grassellino, A. Romanenko, D. A. Sergatskov, "Nitrogen-doped 9-cell cavity performance in a test cryomodule for LCLS-II," *J. Appl. Phys.,* vol. 117, p. 023908, 2015.

[6] M. Martinello, M. Checchin, A. Grassellino, A.C. Crawford, O. Melnychuk, A. Romanenko, A. D. Sergatskov, "Magnetic flux studies in horizontally cooled elliptical superconducting cavities," *J. Appl. Phys.*, vol. 118, p. 044505, 2015.

[7] J-M. Vogt, O. Kugeler, J. Knobloch, "High-Q operation of superconducting rf cavities: Potential impact of thermocurrents on the rf surface resistance," Phys. Rev. ST Accel. Beams 18, 042001(2015).

[8] H. Huang, T. Kubo, R. L. Geng, "Dependence of trapped-flux-induced surface resistance of a large-grain Nb superconducting radio-frequency cavity on spatial temperature gradient during cool down through T_c," *Phys. Rev. Accel. Beams,* vol. 19, p. 082001, 2016.

[9] S. Posen, M. Checchin, A. C. Crawford, A. Grassellino, M. Martinello, O. S. Melnychuk, A. Romanenko, D. A. Sergatskov, Y. Trenikhina, "Efficient expulsion of magnetic flux in superconducting radio frequency cavities for high Q_0 applications," *J. Appl. Phys.,* vol. 119, p. 213903, 2016.

[10] D. Gonnella, J. Kaufman, M. Liepe, "Impact of nitrogen doping of niobium superconducting cavities on the sensitivity of surface resistance to trapped magnetic flux," *J. Appl. Phys.* vol. 119, p. 073904, 2016.

[11] E. H. Brandt, "The flux-line lattice in superconductors," *Rep. Prog. Phys.*, vol. 58, p. 1465, 1995.

[12] A. Gurevich, and G. Ciovati, "Dynamics of vortex penetration, jumpwise instabilities, and nonlinear surface resistance of type-II superconductors in strong rf fields," *Phys. Rev. B*, vol. 77, p. 104501, 2008.

[13] A. Gurevich, "Theory of RF superconductivity for resonant cavities," *Supercond. Sci. Technol.*, vol. 30, p. 034004, 2017.

[14] P. Dhakal, G. Ciovati, and A. Gurevich, Flux expulsion in niobium superconducting radio-frequency cavities of different purity and essential contributions to the flux sensitivity," *Phys. Rev. Accel. Beams*, vol. 23, p. 023102, 2020.

[15] M. Checchin, M. Martinello, A. Grassellino, A. Romanenko, J. F. Zasadzinski, "Electron mean free path dependence of the vortex surface impedance," *Supercond. Sci. Technol*, vol. 30, p. 034003, 2017.

ISBN: 978-3-95450-233-2 ISSN: 2673-5504 doi:10.18429/JACoW-SRF2021-SUPFDV003

[16] R. Willa, V. B. Geshkenbein, and G.Blatter," Campbell penetration depth in the critical state of type-II superconductors," Phys. Rev. B,vol. 92, p. 134501, 2015.

[17] R. Willa, V. B. Geshkenbein, and G. Blatter, "Probing the pinning landscape in type-II superconductors via Campbell penetration depth," *Phys. Rev. B*, vol. 93, p. 064515, 2016.

[18] W. P. M. R. Pathirana and A. Gurevich, "Nonlinear dynamics and dissipation of a curvilinear vortex driven by a strong time-dependent Meissner current," *Phys. Rev. B,* vol. 101, p. 064504, 2020.

[19] W. P. M. R. Pathirana and A. Gurevich, "Effect of random pinning on nonlinear dynamics and dissipation of a vortex driven by a strong microwave current," *Phys. Rev. B*, vol. 103, p. 184518, 2021.

[20] G. Catelani and J. P. Sethna, "Temperature dependence of the super heating field for superconductors in the high -κ London limit," *Phys. Rev. B,* vol. 78, p. 224509, 2008.

[21] F. Pei-Jen Lin and A. Gurevich, "Effect of impurities on the super heating field of type II superconductors," *Phys. Rev. B*, vol. 85, p. 054513, 2012.

[22] A. Sheikhzada and A. Gurevich, "Maximum dynamic pair-breaking current and super fluid velocity in non equilibrium superconductors," *Phys. Rev. B*, vol. 102, p. 104507, 2020.

[23] T. Kubo, "Super fluid flow in disordered superconductors with Dynes pair-breaking scattering: Depairing current, kinetic inductance, and superheating field," *Phys. Rev. Research 2,* p. 033203, 2020.

[24] P. G. DeGennes and J. Matricon, "Collective modes of vortex lines in superconductors of the second kind, *Rev. Mod. Phys*., vol. 36, p. 45, 1964.

[25] N. Lütke-Entrup, B. Placais, P. Mathieu, and Y. Simon, "RF-studies of vortex dynamics in isotropic type-II superconductors, *Physica B,*vol. 255, p. 75, 1998.

[26] S. Vasiliev, V. V. Chabanenko, N. Kuzovoi, V. F. Rusakov, A. Nabialek, and H. Szymczak, "Energy absorption by a single Abrikosov's vortex in NbTi and YBaCuO superconductors, *J. Supercond. Nov. Magn.,* vol.26, p. 2033, 2013.

[27] M. Tinkham, *Introduction to superconductivity*. Courier Corporation, 2004.

[28] G. Blatter, M. V. Feigel'man, V. B. Geshkenbein, A. I. Larkin, and V. M. Vinokur, "Vortices in high temperature superconductors, *Rev. Mod. Phys.*, vol. 66, p. 1125, 1994.

[29] A. M. Campbell and J. E. Evetts, "Flux vortices and transport currents in type-II superconductors," *Adv. Phys*., vol. 21, p. 99, 1972.

[30] L. Embon, Y. Anahory, A. Suhov, D. Halbertal ,J. Cuppens, A. Yakovenko, A. Uri ,Y. Myasoedov, M. L. Rappaport, M. E. Huber, A. Gurevich, and E. Zeldov, "Probing dynamics and pinning of single vortices in superconductors at nanometer scales," *Sci. Rep.,* vol. 5, p. 7598, 2015.

[31] COMSOL Multiphysics Modeling Software, https://www.comsol.com.